MICROROBOTS

Biohybrid microrobots regulate colonic cytokines and the epithelium barrier in inflammatory bowel disease

Zhengxing Li†, Yaou Duan†, Fangyu Zhang†, Hao Luan, Wei-Ting Shen, Yiyan Yu, Nianfei Xian, Zhongyuan Guo, Edward Zhang, Lu Yin, Ronnie H. Fang, Weiwei Gao, Liangfang Zhang*, Joseph Wang*

Cytokines have been identified as key contributors to the development of inflammatory bowel disease (IBD), yet conventional treatments often prove inadequate and carry substantial side effects. Here, we present an innovative biohybrid robotic system, termed "algae-MΦNP-robot," for addressing IBD by actively neutralizing colonic cytokine levels. Our approach combines moving green microalgae with macrophage membrane–coated nanoparticles (MΦNPs) to efficiently capture proinflammatory cytokines "on the fly." The dynamic algae-MΦNP-robots outperformed static counterparts by enhancing cytokine removal through continuous movement, better distribution, and extended retention in the colon. This system is encapsulated in an oral capsule, which shields it from gastric acidity and ensures functionality upon reaching the targeted disease site. The resulting algae-MΦNP-robot capsule effectively regulated cytokine levels, facilitating the healing of damaged epithelial barriers. It showed markedly improved prevention and treatment efficacy in a mouse model of IBD and demonstrated an excellent biosafety profile. Overall, our biohybrid algae-MΦNP-robot system offers a promising and efficient solution for IBD, addressing cytokine-related inflammation effectively.

INTRODUCTION

Inflammatory bowel disease (IBD) represents a major health care challenge characterized by persistent inflammation in the gastrointestinal (GI) tract (*1*, *2*). It stands as one of the most prevalent autoimmune disorders, disrupting the normal functions of the intestinal barrier and perturbing the complex interplay of cytokines and cells in the gut (*1*, *2*). Cytokines are pivotal in orchestrating the intestinal response to conditions such as cancer, infections, and tissue injuries, and they play a central role in the context of IBD (*3*–*5*). Throughout the progression of IBD, activated macrophages (MΦs) produce excessive proinflammatory cytokines, further disturbing intestine mucosal homeostasis and worsening the symptoms (*6*, *7*). Hence, there is a pressing need for innovative anticytokine therapies to regulate cytokine activity and effectively manage IBD (*8*, *9*). Traditional treatments can be effective when targeting specific cytokines, but their effectiveness is limited because of the diverse array of cytokines produced as the disease advances (*10*, *11*). Moreover, the immunosuppressive nature of conventional medications may lead to long-term side effects, potentially disrupting the immune system, causing liver damage, predisposing patients to infections, and increasing the risk of malignancies (*12*). Given the chronic and incurable nature of IBD, its management carries substantial financial implications (*13*).

Over the past decade, actively propelled micro- and nanoscale robots have demonstrated numerous advantages in various biomedical delivery and neutralization applications (*14*–*22*). Compared with earlier microrobot systems such as magnetically powered microrobots (*23*, *24*), chemically powered microrobots (*25*–*29*), or bacteria-based microrobots (*30*–*32*), recent attention has increasingly focused on green algae–based microrobots for biomedical research because of their immunological biocompatibility and safety, prolonged autonomous self-propulsion capabilities with high speed based on onboard actuation, powerful directed tactic locomotion and guidance in response to diverse stimuli, autofluorescence imaging capability, durable and efficient cargo transportation, motion-induced fluid mixing, large-scale production and miniaturization, and their superior distribution and long-term retention in major organs (*22*, *33*–*36*). Advanced functionalities for cargo delivery or toxin neutralization can be readily incorporated into such microrobots through modification of the algae surface with appropriate components. These advantageous characteristics have been underscored in recent applications, such as the use of antibiotic-loaded algae robots for treating ventilator-associated pneumonia, showcasing antibacterial efficacy attributed to their effective immune evasion and rapid dispersion, along with strong retention throughout the lungs (*33*). Algae-based robots have also demonstrated biocompatibility for operating in the GI tract with prolonged retention time and wide distribution (*36*). These promising attributes of algae-based robots hold considerable potential for IBD treatment with appropriate surface modifications.

In this article, we introduce an algae-based robot that is functionalized with MΦ membrane–coated nanoparticles (MΦNPs) and is referred to as "algae-MΦNP-robot" (fig. S1). By combining the dynamic mobility advantages of active microrobots with the versatile functionality of natural cell membrane coatings, cell membrane–functionalized microrobots have demonstrated accelerated biodetoxification processes and enhanced disease treatment compared with their static cell-membrane counterparts (*37*, *38*). Cell membrane coating is a robust technique that imparts nanoparticles with intrinsic cellular functions (*39*, *40*). In particular, biomimetic MΦNPs serve as decoys for MΦs, effectively neutralizing proinflammatory cytokines because of the inclusion of various cytokine receptors found on the membranes of these immune cells (*41*, *42*). By leveraging the endogenous cytokine receptors present on the MΦ cell membrane, the MΦNPs offer a unique approach to effectively

Department of Nanoengineering, University of California San Diego, La Jolla, CA 92093, USA.
*Corresponding author. Email: josephwang@ucsd.edu (J.W.); zhang@ucsd.edu (L.Z.)
†These authors contributed equally to this work.

neutralizing excessive proinflammatory cytokines while not directly suppressing the immune system. Functionalizing self-propelled algae with these cytokine-targeting MΦNPs enables effective movement of these MΦ decoys. Such biomimetic functionalization results in highly motile cytokine receptors capable of "on-the-fly" capture and removal of specific proinflammatory cytokines such as tumor necrosis factor–α (TNF-α), interleukin-6 (IL-6), IL-1β, and interferon-γ (IFN-γ). The resulting mobile algae-MΦNP-robots navigate through the inflamed colon in a dextran sulfate sodium (DSS)–induced murine model, actively binding free cytokines onto the moving MΦ membrane. This accelerated cytokine neutralization process is a result of improved cell membrane–cytokine interactions facilitated by the efficient motion of MΦNP-functionalized algal microrobots and enhanced fluid dynamics in cytokine-rich solutions. The effective microrobot-assisted on-the-fly neutralization of proinflammatory cytokines leads to the rapid moderation of the immune cascade, ultimately restoring regular cellular homeostasis and alleviating the symptoms of IBD.

RESULTS

Preparation and characterization of the algae-MΦNP-robot

To prepare the algae-MΦNP-robot, we first synthesized the MΦ membrane–coated poly(lactic-*co*-glycolic acid) (PLGA) MΦNPs through a previously reported ultrasonic method (*41*). To visualize the structure of MΦNPs, we loaded hydrophobic fluorescence dye 3,3′-dioctadecyloxa-carbocyanine perchlorate (DiO) into a PLGA nanoparticle core and 1,1′-dioctadecyl-3,3,3′,3′-tetramethylindocarbocyanine perchlorate (DiI) onto the MΦ membrane separately. Fluorescence images showed the uniform overlap of the two fluorescence signals, indicating successful membrane coating onto the PLGA cores (fig. S2A). Transmission electron microscopy imaging further verified the core-shell structure of MΦNPs with a membrane layer wrapping around the nanoparticle core (fig. S2B). Upon membrane coating, dynamic light scattering measurements displayed a hydrodynamic size change from 87 to 120 nm (fig. S2C) and a surface zeta potential change from −48 to −18 mV (fig. S2D). The MΦNPs were then labeled with azide–PEG_4–*N*-hydroxysuccinimide (NHS) ester by reacting with the primary amine group on the MΦNP surface. Green microalgae, *Chlamydomonas reinhardtii*, were modified with dibenzocyclooctyne (DBCO)−PEG_4-NHS with a similar approach. After removing the free reagents, azido-modified MΦNPs were conjugated onto the DBCO-modified algae surface through click chemistry (fig. S3). Scanning electron microscopy (SEM) was used to examine conjugation by visualizing the morphological change in the algae-MΦNP-robot (Fig. 1, A and B) compared with bare microalgae (fig. S4). In addition, efficient MΦNP conjugation was confirmed by fluorescence images (Fig. 1C) and flow cytometry analysis, and the binding efficiency between MΦNPs (DiO) and the green algae [cyanine-5 (Cy5)] was determined to be 92.9% (fig. S5).

Speed and motility ratio of the algae-MΦNP-robot

We observed a negligible change in motion speed of the algae-MΦNP-robot at both room temperature (RT; 22°C, 108.6 ± 11.7 μm/s) and body temperature (BT; 37°C, 63.8 ± 15.8 μm/s) in the tris-acetate-phosphate (TAP) culture medium when compared with that of the bare algae at RT (112.9 ± 11.2 μm/s) and BT (60.5 ± 14.1 μm/s), respectively (fig. S6A), indicating that the MΦNP modification did not affect the motility of green algae. We further observed inappreciable differences in the motile ratio (fig. S6B) and algae viability (fig. S6, C and D) between the algae-MΦNP-robot and bare algae at RT or BT. To simulate the robotic motion behavior in a colonic environment, artificial colonic fluid (ACF; pH ~7.8) was prepared. In ACF, the algae-MΦNP-robot showed a stable speed of ~109.4 ± 13.7 μm/s at RT for 12 hours and maintained a speed of 57.0 ± 12.8 μm/s at BT after 12 hours (Fig. 1D and movie S1). Furthermore, we also examined the motility ratio and found that it remained at a high level (>90%) under RT and decreased from 95.8 to 63.0% under BT after 12 hours (Fig. 1E). To observe the movement of the algae-MΦNP-robot, we captured and displayed the representative trajectories at 0-, 1-, and 2-s intervals (fig. S7, A to C, and movie S2), alongside their corresponding mean speed distributions in ACF at 0, 1, and 12 hours at BT (fig. S7, D to F).

To further demonstrate the motility of the algae-MΦNP-robot in the inflamed colon section, we transferred the green algae into cytokine-containing ACF to mimic the colonic condition in inflammatory colitis. The algae-MΦNP-robot remained motile at 115.3 ± 15.6 μm/s in TNF-α–containing ACF, 98.4 ± 14.8 μm/s in IL-6–containing ACF, 104.6 ± 15.8 μm/s in IL-1β–containing ACF, and 96.7 ± 16.1 μm/s in IFN-γ–containing ACF (~10 body lengths/s). The speed dropped to 36.4 ± 11.1, 41.8 ± 9.7, 42.7 ± 10.9, and 53.1 ± 9.6 μm/s under the four cytokine-containing ACF conditions, respectively (~4 body lengths/s), at 12 hours at BT (Fig. 1, F to I, and movie S3). Such behavior was similar to the changes in ACF without cytokines, reflecting a negligible impact of free cytokines on the motility of the algae-MΦNP-robot. Similarly, the algae-MΦNP-robot motile ratio was examined in each cytokine-containing solution. After 12 hours at BT, the green algae motile ratio was preserved at 55.3% for TNF-α, 65.2% for IL-6, 58.6% for IL-1β, and 52.9% for IFN-γ (Fig. 1, J to M). Furthermore, the algae-MΦNP-robot viability ratio remained at 87.0% for TNF-α, 85.3% for IL-6, 87.2% for IL-1β, and 83.7% for IFN-γ (fig. S8). The effect of TNF-α on the motile ratio of green algae was significantly different from the effects of other cytokines (fig. S9, A and B). Overall, these findings showed that most of the algae-MΦNP-robots exhibited proficient movement in a cytokine-rich environment associated with inflamed colitis regions.

In vitro cytokine neutralization capacity of the algae-MΦNP-robot

We first quantified the loading efficiency of MΦNPs in the algae-MΦNP-robot formulation. It showed a maximum loading of ~150 μg of MΦNPs conjugated onto 1×10^7 algae while maintaining the peak motility of algae (Fig. 2A and fig. S10). We also prepared MΦNP-modified deflagellated algae (denoted as "static algae-MΦNPs") that do not have a motile function as a control. The morphology of static algae-MΦNPs was characterized by SEM (fig. S11). Next, we performed Western blotting to characterize the MΦ membrane receptors including TNF-α receptor (TNF-R1), IL-6 receptor (IL-6Rα), IL-1β receptor (IL-1Rl), and IFN-γ receptor (IFN-γRα) (*42*) on all experimental samples, including MΦ membrane vesicles, free MΦNPs, algae-MΦNP-robot, static algae-MΦNPs, and bare algae (Fig. 2B). To evaluate the cytokine neutralization capacity, we mixed all of the experimental groups with TNF-α, IL-6, IL-1β, and IFN-γ, which play crucial roles in inducing IBD and promoting disease progression. As shown in Fig. 2 (C to F), under the same concentration of MΦNPs, the algae-MΦNP-robot offered a markedly enhanced cytokine neutralization capability compared with static

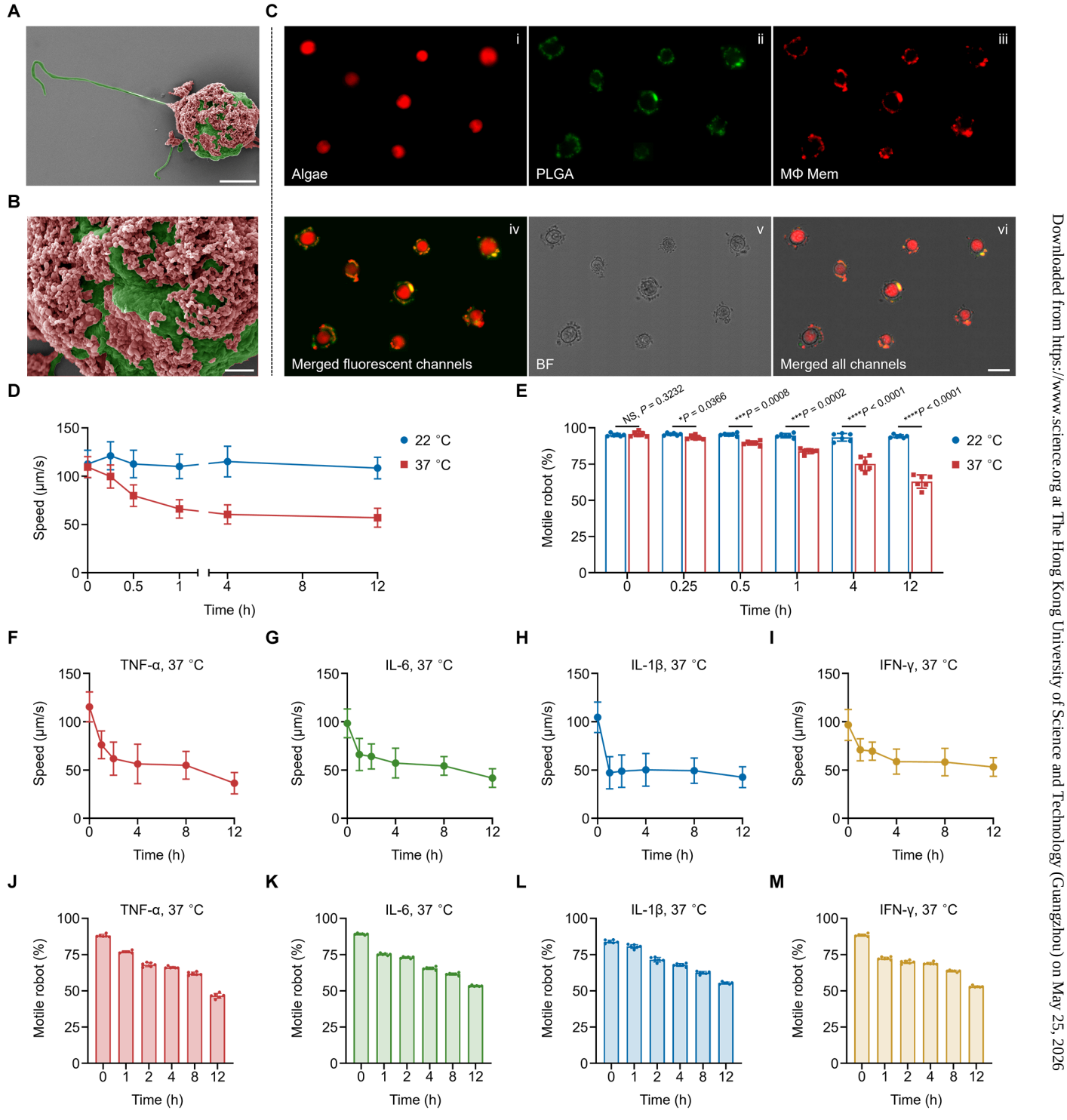

Fig. 1. Characterization and motility of the algae-MΦNP-robot. (**A**) Representative SEM images of the algae-MΦNP-robot. Scale bar, 5 μm. (**B**) Zoomed-in SEM image of (A) showing the MΦNPs attaching to the green algae surface. Scale bar, 1 μm. (**C**) Bright-field and fluorescence images of the algae-MΦNP-robot. (i) Autofluorescence of algae chloroplast in the Cy5 channel; (ii) DiO-labeled PLGA core in the GFP channel; (iii) DiI-labeled MΦ membrane in the RFP channel; (iv) merged image from all three fluorescence channels; (v) bright-field image of the algae-MΦNP-robot; and (vi) merged image from all channels. Scale bar, 10 μm. (**D** and **E**) The speed (D) and motile robot ratio (E) of the algae-MΦNP-robot in ACF at RT (22°C) and BT (37°C), respectively [(D) $n = 100$, error bars represent ±SD relative to the mean; (E) $n = 6$, error bars represent ±SD relative to the mean] (movie S1). (**F** to **I**) Speed changes in the algae-MΦNP-robot in ACF with different cytokines, including TNF-α (F) (1 ng/ml), IL-6 (G) (10 ng/ml), IL-1β (H) (10 ng/ml), and IFN-γ (I) (3.5 ng/ml) at BT (37°C, $n = 100$, error bars represent ±SD relative to the mean). (**J** to **M**) Motile ratio changes in the algae-MΦNP-robot in ACF with different cytokines, including TNF-α (J) (1 ng/ml), IL-6 (K) (10 ng/ml), IL-1β (L) (10 ng/ml), and IFN-γ (M) (3.5 ng/ml) at BT (37°C, $n = 6$, error bars represent ±SD relative to the mean). Statistical analysis for the motile ratio was performed using a paired two-tailed *t* test. NS: $P > 0.05$, $^{*}P \leq 0.05$, $^{***}P \leq 0.001$, and $^{****}P < 0.0001$.

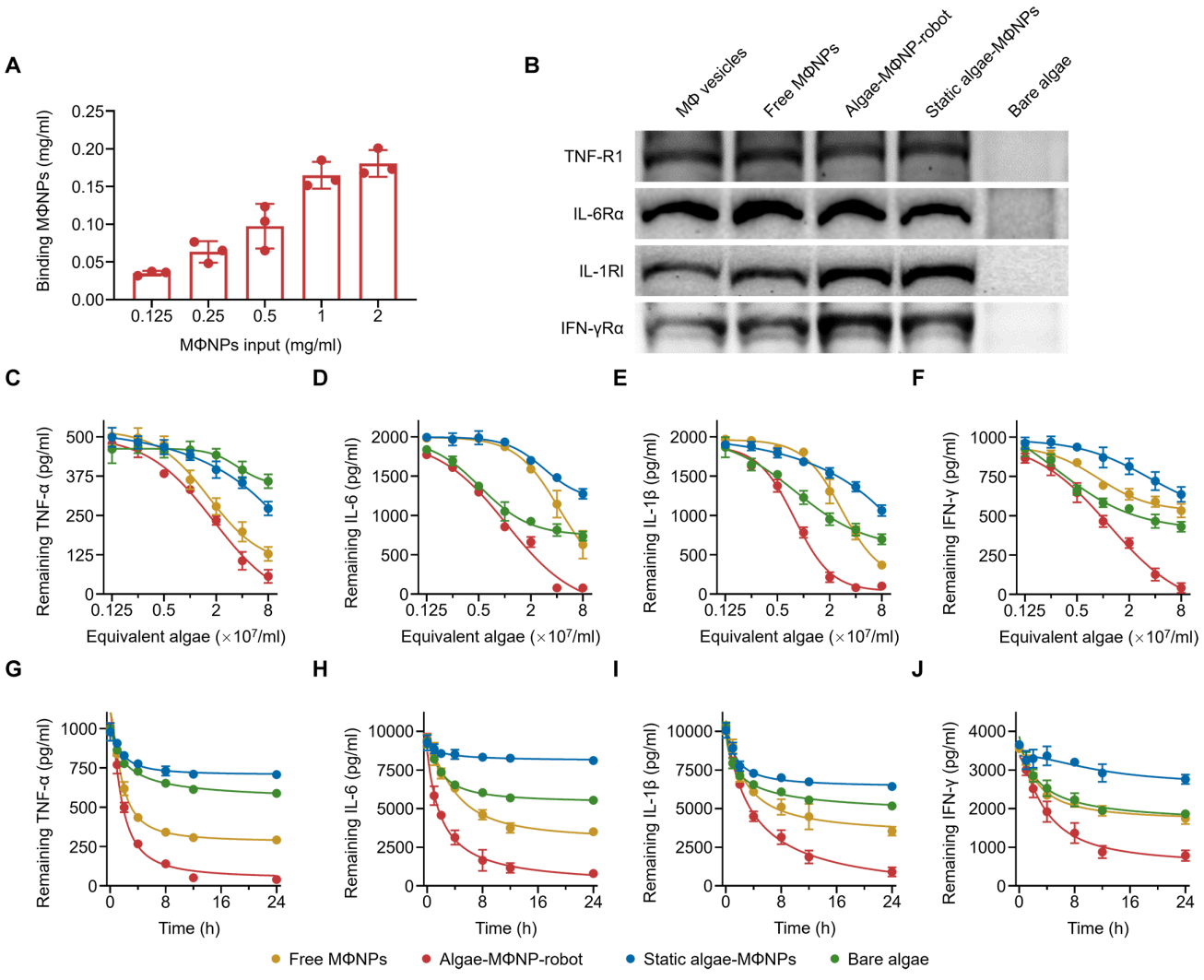

Fig. 2. In vitro cytokine neutralization efficacy of the algae-MΦNP-robot. (**A**) Quantification of different inputs of MΦNPs binding to 1×10^7/ml algae ($n = 3$; error bars represent ±SD relative to the mean). (**B**) Representative cytokine receptor bands on MΦ membrane vesicles, free MΦNPs, algae-MΦNP-robot, static algae-MΦNPs, and bare algae resolved by Western blotting. (**C** to **F**) Neutralization of TNF-α (C), IL-6 (D), IL-1β (E), and IFN-γ (F) at BT (37°C) with different concentrations of free MΦNPs (yellow), algae-MΦNP-robot (red), static algae-MΦNPs (blue), and bare algae (green) at an equivalent concentration of MΦNPs (0.15 mg/ml) binding to 1×10^7/ml algae ($n = 3$, error bars represent ±SD relative to the mean). (**G** to **J**) Time-dependent neutralization of TNF-α (G), IL-6 (H), IL-1β (I), and IFN-γ (J) at BT (37°C) with free MΦNPs [yellow; MΦNPs (0.6 mg/ml)], algae-MΦNP-robot [red; MΦNPs (0.6 mg/ml) binding to algae robot (4×10^7/ml)], static algae-MΦNPs [blue; MΦNPs (0.6 mg/ml) binding to static algae (4×10^7/ml)], and bare algae [green; bare algae (4×10^7/ml)] ($n = 3$; error bars represent ±SD relative to the mean). The nonlinear fit curve for (C) to (J) was performed using a variable slope (four parameters) model through GraphPad Prism 9.

algae-MΦNPs, reflecting the dynamic motility of the microrobot. Moreover, the algae-MΦNP-robot exhibited exceptional neutralization ability when compared with its individual components, surpassing the bare algae because of the specific receptors obtained from MΦNPs. Compared with free MΦNPs, the algae-MΦNP-robot allowed for continuous movement of MΦNPs, thereby increasing the receptor-cytokine binding efficacy. Such on-the-fly interactions with the algae-MΦNP-robot greatly accelerated the neutralization process under the same receptor concentration. To analyze the neutralization kinetic profiles, we determined the half-maximal inhibitory concentration value of the algae-MΦNP-robot for binding TNF-α, IL-6, IL-1β, and IFN-γ to be 1.870×10^7, 1.042×10^7, 0.7870×10^7, and 1.167×10^7/ml, respectively, based on the Hill equation (fig. S12). Then, we incubated 15 μg of MΦNPs (corresponding to 1×10^6 green algae) with the four different cytokines for 24 hours to further study the neutralization capacity. Upon mixing with a higher dosage of free cytokines, the algae-MΦNP-robot neutralized 94.8% of TNF-α, 87.7% of IL-6, 81.9% of IL-1β, and 75.6% of IFN-γ within 12 hours at BT, indicating a substantial improvement compared with free MΦNPs (69.2% of TNF-α, 60.9% of IL-6, 56.0% of IL-1β, and 45.2% of IFN-γ) and static algae-MΦNPs (29.3% of TNF-α, 10.7% of IL-6, 33.0% of IL-1β, and 19.9% of IFN-γ) (Fig. 2, G to J). We further verified that the algae-MΦNP-robot could effectively neutralize a mixture of four types of cytokines (fig. S13). Collectively, these in vitro cytokine neutralization results demonstrated that the algae-MΦNP-robot formulation displayed

rapid and efficient cytokine neutralization, suggesting high potential for effective treatment of inflammatory colitis.

In vivo protection, release, and retention in the GI tract

To facilitate the delivery of our algae-MΦNP-robot to the colonic area, we established an oral administration capsule formulation. Briefly, we shortened the length of the commercial capsule body from 7 to 4 mm to ensure easy passage through the stomachs of mice (fig. S14A). To maintain the motility and viability of the algae-MΦNP-robot, we created a hydrophobic layer on the inner side of the capsule by applying a mixture of 4% octadecyltrimethoxysilane (OTMS) in pure ethanol as reported previously (*43*, *44*) (fig. S14B). The loaded algae-MΦNP-robot exhibited proper Cy5 fluorescence throughout the entire capsule, as observed under the corresponding microscopy channel [excitation/emission (ex/em) = 647 nm/680 nm], reflecting the autofluorescence of the green algae (fig. S14C). To ensure capsule stability in the acidic stomach environment and targeted delivery to the colonic area (pH ~7.5), we coated a pH-responsive Eudragit S-100 enteric coating material on the outside of the capsule. Under simulated in vivo conditions, we evaluated the release profile of the capsule loaded with the algae-MΦNP-robot (denoted as "algae-MΦNP-robot capsule") in simulated gastric fluid (SGF) and ACF at BT under 400 rpm of stirring (to mimic the localized natural convection). The results illustrated that capsules without enteric coating dissolved in the SGF within 30 min (fig. S15A). In comparison, the capsules with enteric coating remained protected for more than 3 hours in SGF and released ~90% of their content within 30 min in ACF (fig. S15B). Furthermore, we collected and characterized the green algae released in the SGF and ACF and found that when the algae-MΦNP-robot was released in SGF, it caused damage to the green algae body, resulting in a loss of the cytokine neutralization ability compared with the green algae released into ACF (fig. S16). In addition, after being released from the capsule, the algae-MΦNP-robot maintained a stable motion speed of 69.8 ± 15.8 μm/s with a motility ratio of ~61.6% (fig. S17) at BT.

To investigate the in vivo functionality of the algae-MΦNP-robot capsule (Fig. 3A), we used a fluorescent dye, 1,1′-dioctadecyl-3,3,3′,3′-tetramethylindotricarbocyanine iodide (DiR; ex/em = 748 nm/780 nm), to label the PLGA core of the algae-MΦNP-robot for in vivo visualization and to minimize the background fluorescence from tissues. For oral administration, we loaded 2×10^6 algae-MΦNP-robots and static algae-MΦNPs into their corresponding capsules and quantified the average radiant signal using the IVIS Cy7 channel (fig. S18). After feeding the capsules to 7-week-old C57BL/6 mice, we collected their GI systems at different time points and observed them using IVIS. We observed a condensed fluorescence signal and the undamaged capsule after opening the tissue at the signal position (Fig. 3B and fig. S19). Analyzing the average radiant signal from the algae-MΦNP-robot–loaded capsules in the stomach and small intestine, we found no significant difference $P = 0.6524$ and $P = 0.9730$) when compared with the algae-MΦNP-robot–loaded capsule before oral administration, indicating that our capsule formulation was able to protect the algae-MΦNP-robot upon passage through the harsh stomach environment toward the small intestine (Fig. 3C). Furthermore, we collected and dissolved the capsules from the stomach and small intestine in ACF and confirmed that the released algae-MΦNP-robot maintained speeds of 62.9 ± 14.0 and 65.4 ± 13.4 μm/s (fig. S20A and movie S4) with motility ratios of ~59.5 and ~ 57.5% (fig. S20B) and algae viability ratios of ~98.3 and ~ 97.7% (fig. S20, C and D), respectively.

Next, we studied the release and retention of the capsule in the colonic area. The fluorescence from the algae-MΦNP-robot and the static algae-MΦNPs was detected throughout the colonic tissue around 5 hours after oral gavage (Fig. 3D). By monitoring the retention of the algae-MΦNP-robot and the static algae-MΦNPs over time, we observed that the fluorescence signal in the static algae-MΦNP group decreased to 5 and 1% at 7 and 9 hours, respectively (Fig. 3E and fig. S21). However, the algae-MΦNP-robot group maintained 75 and 25% of the signal at 7 and 9 hours, respectively. These results indicated that the motile ability of the algae-MΦNP-robots was effective in prolonging their tissue retention time because the motion in the colon not only increased the chance of the algae microrobots to attach to the colon wall but also reduced their chance of being excreted quickly from the colon.

In vivo prevention efficacy against IBD

The efficacy of the algae-MΦNP-robot to protect and moderate colon destruction was first evaluated through a murine model of DSS-induced acute IBD. Specifically, 7-week-old C57BL/6 mice were supplied with drinking water and administered phosphate-buffered saline (PBS) as the positive control or 3% DSS in drinking water for 6 days and simultaneously administered the algae-MΦNP-robot capsule or various controls [PBS, capsule loaded with static algae-MΦNPs (static algae-MΦNP capsule), and algae-MΦNP-robot without capsule] by daily oral administration (Fig. 4A). The mechanism of action of the algae-MΦNP-robot is different from those of clinically approved drugs for IBD. Thus, no clinical drug was used as a control in the in vivo studies. During the administration, we monitored mouse body weight and disease activity index (DAI) daily. The results indicated that the algae-MΦNP-robot capsule treatment alleviated the abnormality caused by DSS-induced colitis effectively (Fig. 4, B and C). Compared with the static algae-MΦNP capsule, the continuous motion of algae-MΦNP-robot conferred a prolonged distribution in the target region, resulting in a more efficient treatment effect. Under an identical algae-MΦNP-robot dosage, the capsule formulation showed a more profound efficacy than the capsule-free control counterpart. Such improvement reflects the protection of the algae-MΦNP-robots by the capsule from the harsh stomach environment to maintain their motility and cytokine neutralization abilities. On day 10, the mice were euthanized for tissue collection and analysis. By comparing with other control groups, only the algae-MΦNP-robot capsule group predominantly maintained the colon length of the mice at a level comparable to that of the healthy control (Fig. 4D and fig. S22).

After the homogenization of colonic tissue, we measured the levels of relevant proinflammatory cytokines (TNF-α, IL-6, IL-1β, and IFN-γ) in the colonic tissue. The results showed the effective neutralization capability of the algae-MΦNP-robot capsule against local proinflammatory cytokines, thereby modulating the IBD symptoms. Such capability is attributed to the long-lasting motion of the algae-MΦNP-robot, the protection provided by the capsule, and the effective capture of multiple proinflammatory cytokines (Fig. 4E). To further examine the status of the colonic tissue, we conducted hematoxylin and eosin (H&E) staining analysis (Fig. 4F) and terminal deoxynucleotidyl transferase–mediated deoxyuridine triphosphate nick end labeling (TUNEL) assay (fig. S23). The H&E staining analysis provided a direct evaluation of the colonic damage, which

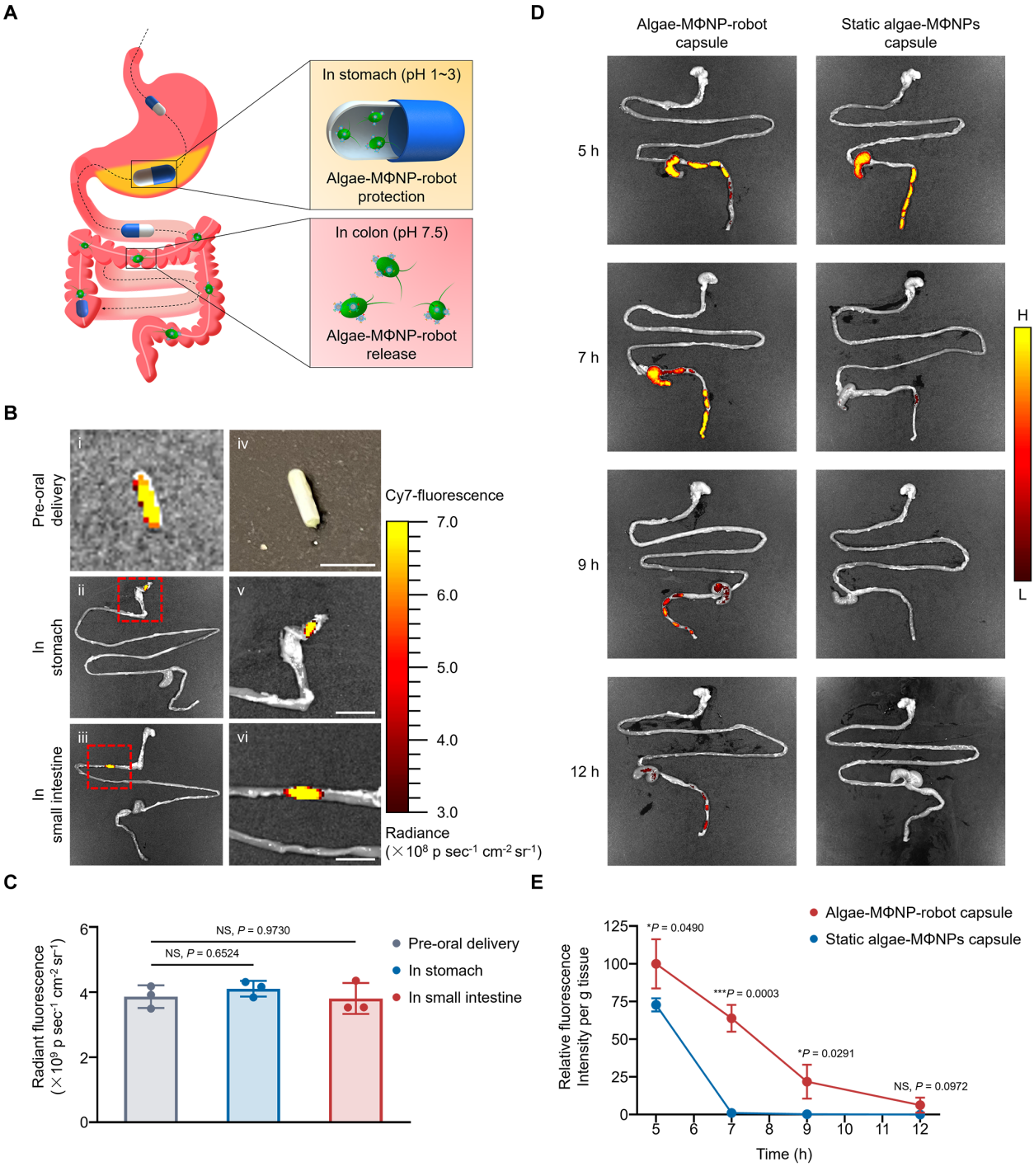

Fig. 3. In vivo characterization of the algae-MΦNP-robot capsule in the GI tract. (**A**) Schematic of the algae-MΦNP-robot capsule in the GI tract. The capsules protect the algae-MΦNP-robot in the stomach from exposure to the extreme acid environment and release the algae-MΦNP-robot in the colonic area. (**B**) Ex vivo IVIS fluorescence images of GI tissues showing the capsule-protected algae-MΦNP-robot (i, ii, and iii) and the zoomed-in view of the capsules (iv, v, and vi). Scale bars, 5 mm. (**C**) Comparison of fluorescence intensity of the capsules before oral delivery in the stomach or small intestine from (B) ($n = 3$, error bars represent ±SD relative to the mean). (**D**) Ex vivo fluorescence images of GI tissues at different time points (5, 7, 9, and 12 hours) after oral administration of the algae-MΦNP-robot capsule or static algae-MΦNP capsule (negative control) (H, high signal; L, low signal). (**E**) Quantified relative fluorescence intensity per gram of colonic tissues collected in (D) ($n = 3$, error bars represent ±SD relative to the mean). Statistical analysis of the fluorescence comparison among preoral delivery, in the stomach, and in the small intestine (C) was performed using repeated-measures one-way ANOVA. Analysis of the relative fluorescence comparison between the algae-MΦNP-robot capsule and the static algae-MΦNP capsule (E) was performed using a paired two-tailed *t* test. NS: $P > 0.05$, $^{*}P \leq 0.05$, and $^{***}P \leq 0.001$.

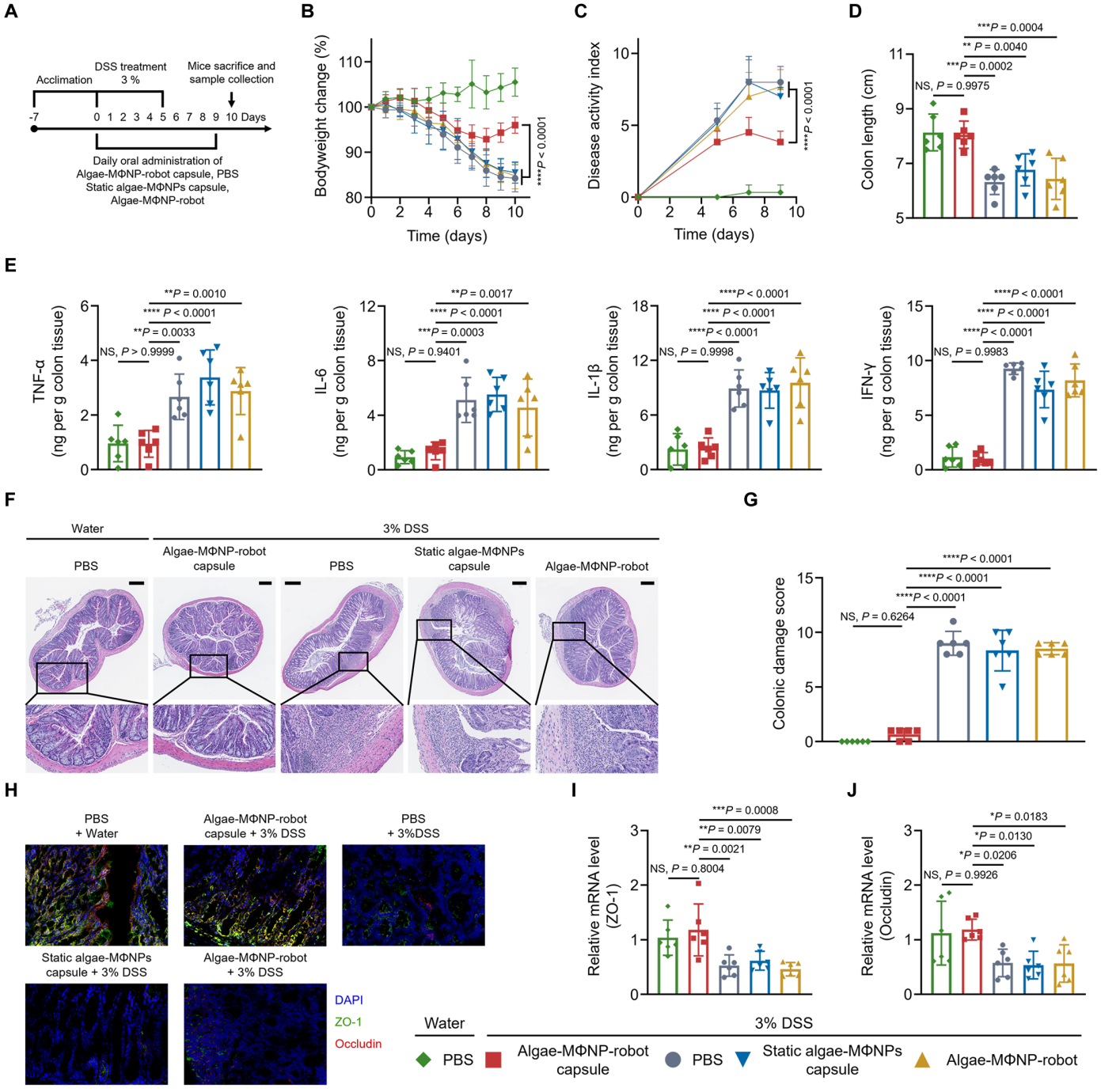

Fig. 4. In vivo prevention efficacy of the algae-MΦNP-robot capsule in a DSS-induced IBD mouse model. (**A**) C57BL/6 mice were provided with water or 3% DSS–containing water for 6 days. Starting from days 0 to 9, mice were orally administered the algae-MΦNP-robot capsule, static algae-MΦNP capsule, algae-MΦNP-robot, or PBS. Mice were then euthanized, and the colonic tissues were collected on day 10. (**B**) Daily mouse body weight changes in each group from days 0 to 10. Data were normalized as a percentage of the body weight on day 0 ($n = 6$, error bars represent ±SD relative to the mean). (**C**) On days 0, 5, 7, and 9, mouse changes in DAI ($n = 6$, error bars represent ±SD relative to the mean). (**D**) Comparison of the mouse colon length in each experimental group ($n = 6$, error bars represent ±SD relative to the mean). (**E**) Concentrations of proinflammatory cytokines (TNF-α, IL-6, IL-1β, and IFN-γ) in the colonic tissues ($n = 6$, error bars represent ±SD relative to the mean). (**F**) H&E staining analysis of colonic sections of each group. Scale bars, 200 μm. (**G**) Colonic damage score of (F) ($n = 6$, error bars represent ±SD relative to the mean). (**H** to **J**) Colonic tissues were excised and analyzed for the related protein expression patterns (H) and related mRNA levels of ZO-1 (I) and occludin (J) ($n = 6$, error bars represent ±SD relative to the mean). The displayed images are representative of $n = 6$ biologically independent animals from two independent experiments. NS, nonsignificant, with $P > 0.05$, $^{*}P \leq 0.05$, $^{**}P \leq 0.01$, $^{***}P \leq 0.001$, and $^{****}P < 0.0001$. Statistical analysis was performed using repeated-measures ANOVA.

verified that the algae-MΦNP-robot capsule group outperformed in all criteria, indicating its effective protection of the colonic tissue and reduction in colon damage (Fig. 4G and fig. S24). The TUNEL assay assessed the viability of epithelium cells, providing valuable insights into the beneficial effect of the algae-MΦNP-robot capsule from a viability perspective. A more detailed examination was also carried out through the study of tight junction protein expression patterns (Fig. 4H) and two related mRNA levels of ZO-1 and occludin (Fig. 4, I and J). Collectively, the algae-MΦNP-robot capsule restored the disrupted colonic epithelium cell layer induced by acute IBD effectively.

In vivo treatment efficacy against IBD

To further study the ability of the algae-MΦNP-robot capsule to ameliorate colitis, we examined it through a delayed treatment regimen in the murine model of DSS-induced IBD. In this study, 7-week-old C57BL/6 mice were given drinking water and administered PBS as the positive control or 3% DSS in drinking water for 6 days to induce acute colitis. After the establishment of acute colitis, the animals were orally administered the algae-MΦNP-robot capsule or controls (PBS, static algae-MΦNP capsule, and algae-MΦNP-robot without capsule) from days 5 to 9 (Fig. 5A). When compared with the control groups, mice treated with the algae-MΦNP-robot capsule exhibited a gradual slowdown in the decrease in body weight, followed by a subsequent increase in body weight (Fig. 5B). In addition, the DAI showed that the administration of the algae-MΦNP-robot capsule could reduce fecal bleeding and improve stool consistency (Fig. 5C). The analysis of the colonic tissue also showed that the algae-MΦNP-robot capsule preserved the colon length and prevented it from further shortening as compared with the control groups (Fig. 5D and fig. S25). Furthermore, the algae-MΦNP-robot capsule group showed the lowest proinflammatory cytokine levels compared with the other treatment groups (Fig. 5E). Specifically, the H&E staining indicated successful regulation and restoration to damaged colonic tissue by the algae-MΦNP-robot capsule (Fig. 5, F and G, and fig. S26). After comparison of the tight junction protein expression patterns (Fig. 5H) and related mRNA levels of ZO-1 and occludin (Fig. 5, I and J), we noticed that the strong fluorescence signals and the comparable mRNA expression levels of ZO-1 and occludin between the healthy group and the algae-MΦNP-robot capsule group indicated an intact epithelial layer and high treatment efficiency.

In vivo acute toxicity study

Last, to evaluate the biosafety of the orally administered algae-MΦNP-robot capsule, we fed the mice daily with one capsule for 10 days (Fig. 6A). In comparison with the PBS control group, we observed no difference in the daily body weight changes in mice administered the algae-MΦNP-robot capsules (Fig. 6B). After a comprehensive analysis of blood chemistry and major blood cell population after oral administration, the algae-MΦNP-robot capsule oral administration did not show any influence on the blood physiology (Fig. 6, C and D). To assess potential tissue-level damage, we studied the various major sections of the GI tract (stomach, duodenum, jejunum, ileum, proximal colon, and distal colon) through H&E staining. No anomalies were observed in these tissues (Fig. 6E). In addition, the heart, kidney, liver, lung, and spleen were also analyzed through H&E staining and showed no abnormal conditions (Fig. 6F). Furthermore, the algae-MΦNP-robot capsule group and the PBS control group showed comparable colonic proinflammatory cytokine levels (Fig. 6G). These findings indicated the favorable biosafety profile of the algae-MΦNP-robot capsule formulation and its oral administration route.

DISCUSSION

We have developed a robust biohybrid robotic platform by combining algae with MΦNPs to actively target and neutralize proinflammatory cytokines. One of the key findings of our research is the highly efficient on-the-fly neutralization of a wide range of cytokines. This achievement results from the synergistic combination of the dynamic movement of biohybrid microrobots and the cytokine-binding properties of MΦNPs. By loading the algae-MΦNP-robot into a capsule for oral delivery to the colon, we observed promising efficacy in both prevention and delayed treatment regimens in a murine model of DSS-induced IBD. Compared with previous studies that used nanoparticles solely as drug carriers for colon cancer or colitis treatment (*11*, *45*), our green algae–based microrobots exhibited superior tissue retention capabilities. This prolonged retention can be attributed to the inherent long-lasting self-propulsion behavior of these microrobots, making them a preferred choice for delivering therapeutic agents. Compared with the static algae-MΦNPs, our active algae-MΦNP-robot demonstrated a broader, more uniform, and sustained distribution throughout the colonic tissue because of their motility. Furthermore, we conducted a comprehensive assessment of the biosafety of the algae-MΦNP-robot capsule. During a 10-day period of daily oral administration, the formulation had no obvious impact on the mice's body weights, blood chemistry, blood cell counts, and GI tissues when compared with the control group, confirming its excellent biosafety profile.

The use of the MΦ membrane in the algae-MΦNP-robot offers several advantages compared with traditional anticytokine therapies. MΦs play a pivotal role in the inflammatory cascade of IBD, making their membrane an ideal choice for efficiently binding and neutralizing cytokines. Therefore, this cytokine-capturing process offers distinct features, including broad-spectrum activity and simplicity, without the complexity associated with traditional fabrication methods. In addition, the MΦ membrane ensures biosafety because it exhibits negligible toxicity, leading to minimal side effects and reduced risk of drug resistance during IBD treatment. When combined with the dynamic green algae robot carrier, MΦNPs achieved even greater neutralization efficiency because the rapidly moving MΦNPs could more effectively capture free cytokines.

The robust capabilities of this algae-MΦNP-robot system not only make it suitable for alleviating IBD symptoms but also position it as a potential solution for addressing other proinflammatory cytokine–related disorders because of its reliable biosafety, high treatment efficiency, and low toxicity. Moreover, the platform's scalability makes it a compelling candidate for future clinical translation, offering the possibility of widespread accessibility. Overall, this algae-MΦNP-robot system has potential for treating inflammatory disorders in a natural and highly effective manner. Moreover, by loading therapeutic payloads onto the algae-MΦNP-robot, it may also be applied for the treatment of other GI disorders, such as gastritis, in which an external field may be integrated to provide further directional control of the microrobots for more accurate localized drug delivery applications. Looking forward, the use of green algae–based biohybrid microrobots for practical applications in

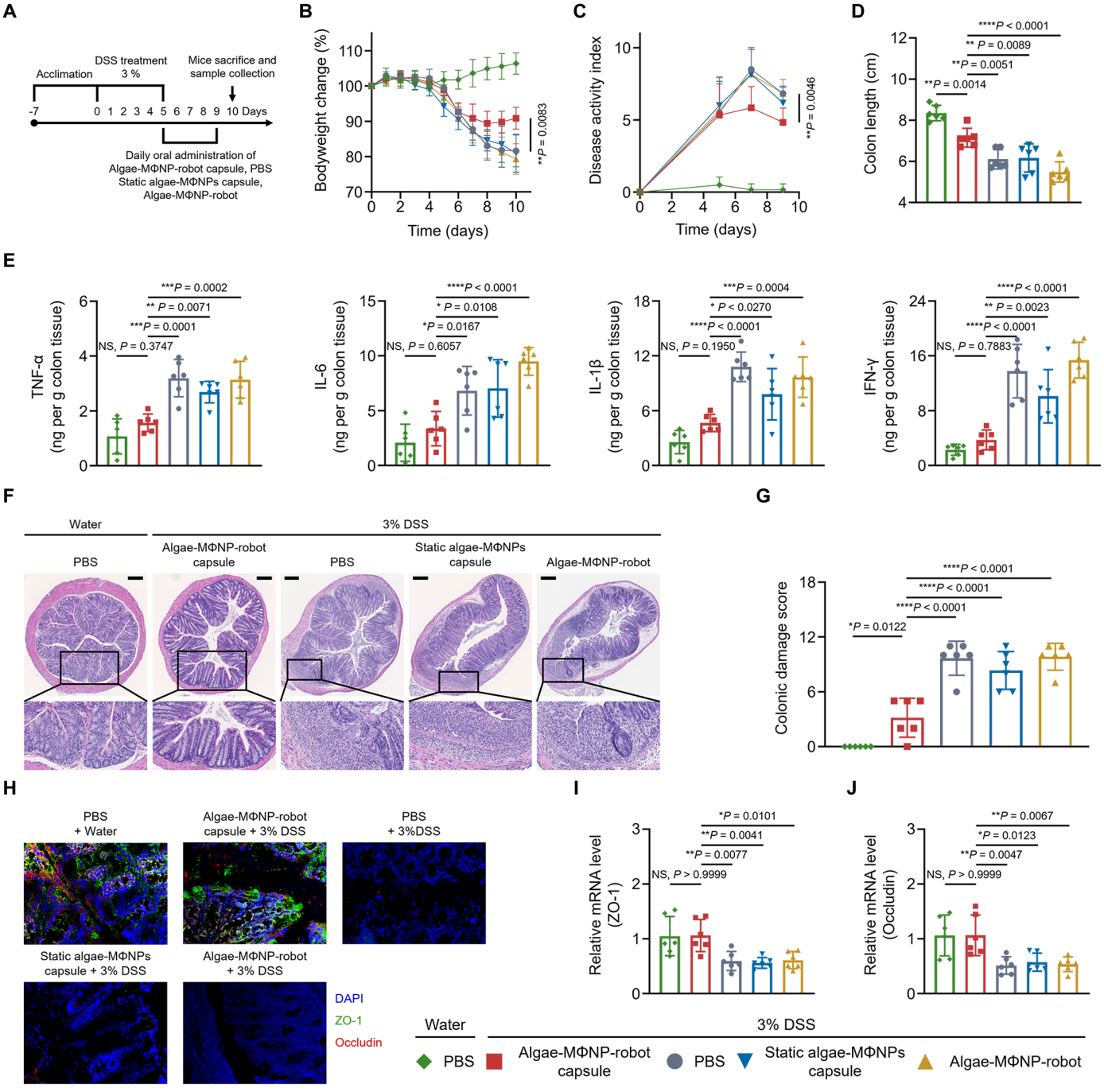

Fig. 5. In vivo treatment efficacy of algae-MΦNP-robot capsule in a DSS-induced IBD mouse model. (**A**) C57BL/6 mice were provided with water or 3% DSS–containing water for 6 days. Starting from days 5 to 9, mice were orally administered the algae-MΦNP-robot capsule, static algae-MΦNP capsule, algae-MΦNP-robot, or PBS. Mice were then euthanized, and the colonic tissues were collected on day 10. (**B**) Daily mouse body weight changes in each group from days 0 to 10. Data were normalized as a percentage of the body weight at day 0 ($n = 6$, error bars represent ±SD relative to the mean). (**C**) On days 0, 5, 7, and 9, mouse changes in DAI ($n = 6$, error bars represent ±SD relative to the mean). (**D**) Comparison of the mouse colon length of each experimental group ($n = 6$, error bars represent ±SD relative to the mean). (**E**) Colonic tissues were analyzed for the concentration of proinflammatory cytokines (TNF-α, IL-6, IL-1β, and IFN-γ) ($n = 6$, error bars represent ±SD relative to the mean). (**F**) H&E staining analysis of colonic sections of each group. Scale bars, 200 μm. (**G**) Colonic damage score of (F) ($n = 6$, error bars represent ±SD relative to the mean). (**H** to **J**) Colonic tissues were excised and analyzed for the related protein expression patterns (H) and related mRNA levels of ZO-1 (I) and occludin (J) ($n = 6$, error bars represent ±SD relative to the mean). The displayed images are representative of $n = 6$ biologically independent animals from two independent experiments. NS, nonsignificant, with $P > 0.05$, $*P \leq 0.05$, $**P \leq 0.01$, $***P \leq 0.001$, and $****P < 0.0001$. Statistical analysis was performed using repeated-measures ANOVA.

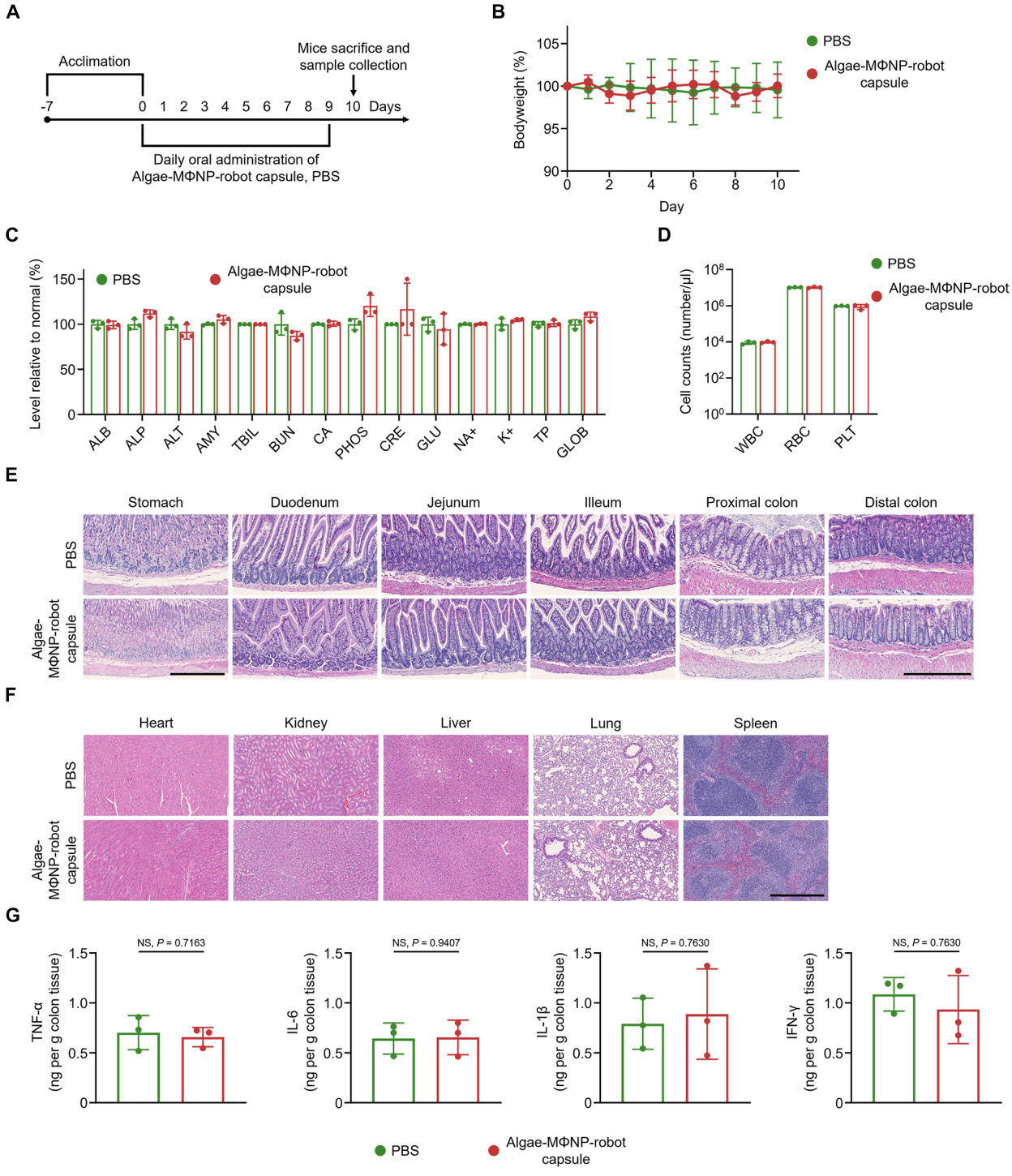

Fig. 6. In vivo biosafety evaluation of the algae-MΦNP-robot capsule. (**A**) C57BL/6 mice were orally administered the algae-MΦNP-robot capsule or PBS from days 0 to 10. Mice were then euthanized, and the blood and related tissue samples were collected on day 10. (**B**) Daily mouse body weight changes in each group from days 0 to 10. Data were normalized as a percentage of the body weight at day 0 ($n = 3$, error bars represent ±SD relative to the mean). (**C**) Comprehensive blood chemistry panel on day 10 after daily oral administration ($n = 3$; error bars represent ±SD relative to the mean). ALB, albumin; ALP, alkaline phosphatase; ALT, alanine transaminase; AMY, amylase; TBIL, total bilirubin; BUN, blood urea nitrogen; CA, calcium; PHOS, phosphorus; CRE, creatinine; GLU, glucose; Na^+, sodium; K^+, potassium; TP, total protein; GLOB, globulin. (**D**) Counts of various blood cells on day 10 after daily oral administration ($n = 3$, error bars represent ±SD relative to the mean). WBC, white blood cells; RBC, red blood cells; PLT, platelets. (**E**) Representative H&E-stained histological sections of different GI sections on day 10 after daily oral administration. Scale bars, 500 μm (stomach) and 300 μm. (**F**) Representative H&E-stained histological sections of major organs, including the heart, kidney, liver, lung, and spleen, on day 10 after daily oral administration. Scale bar, 500 μm. (**G**) Colonic tissues were analyzed for the concentration of proinflammatory cytokines (TNF-α, IL-6, IL-1β, and IFN-γ) ($n = 3$, error bars represent ±SD relative to the mean). Statistical analysis for the motile ratio was performed using a paired two-tailed t test. NS, $P > 0.05$.

humans presents both promising opportunities and challenges. These microrobots offer distinctive functionalities that surpass what passive systems can provide. However, attention must be given to potential contamination, the stability of algae-based products, and maintenance of batch-to-batch consistency during clinical translation. Notably, the reported algae-MΦNP-robot capsule necessitates meticulous formulation optimization for further advancement in practical applications.

MATERIALS AND METHODS

Green algae culture

C. reinhardtii (CC-125 wild-type mt+) was acquired from the Chlamydomonas Resource Center. It was grown in TAP medium (Thermo Fisher Scientific) at RT (~22°C) with alternating cycles of 12 hours of sunlight and 12 hours of darkness.

MΦ cell membrane derivation

J774A.1 murine MΦs (American Type Culture Collection or ATCC, TIB-67) were cultured in Dulbecco's modified Eagle's medium (Invitrogen) supplemented with 10% (v/v) fetal bovine serum (FBS; HyClone, SH30541.03) and 1% (v/v) penicillin-streptomycin (Gibco, 15140122). The cells were maintained in a cell culture incubator at 37°C with 5% CO_2. The cell membrane was derived by following a previously published procedure (*42*). Briefly, frozen cells were thawed and washed three times with 1× PBS using centrifugation at 500*g* for 10 min. The cells were then resuspended in a buffer containing 30 mM tris-HCl (pH 7.5), 225 mM D-mannitol, 75 mM sucrose, 0.2 mM EGTA, and phosphatase/protease inhibitor mixtures (all from MilliporeSigma). The cells were homogenized with a Kinematica POLYTRON PT-10/35 probe homogenizer. The homogenate was centrifuged at 3200*g* for 5 min to remove large debris, leaving behind cell membrane in the supernatant. Then, the sample was centrifuged at 100,000*g* for 35 min at 4°C, and the membrane was collected as pellets. Membrane protein was quantified with bicinchoninic acid assay (BCA, Life Technologies). The cell membrane was kept at −80°C for future studies.

Fabrication of MΦNPs

MΦNPs were synthesized by following a previously published protocol (*42*). First, the polymeric cores were prepared with a nanoprecipitation method. Briefly, 20 mg of PLGA (50:50; 0.67 dl/g; Lactel Absorbable Polymers) was dissolved in 1 ml of acetone. Then, the polymer solution was added dropwise into 1 ml of 10 mM tris buffer (Sigma-Aldrich). The mixture was vacuumed for 1 hour to fully evaporate the acetone. For labeling PLGA cores with fluorescence, 4 μl of DiO (ex/em = 484/501 nm; Thermo Fisher Scientific) or 4 μl of DiR (ex/em = 748/780 nm; Thermo Fisher Scientific) was mixed with 1 ml of acetone containing 20 mg of PLGA. The solution was used to prepare the cores following the same procedure. After the core synthesis, the PLGA cores were mixed with J774A.1 membrane at a 1:1 polymer-to-protein weight ratio. The mixture was sonicated for 3 min with a bath sonicator (Fisherbrand 11201 series, Thermo Fisher Scientific). The sample was washed five times with ultrapure water at 16,100*g* for 5 min and suspended in ultrapure water for future use.

Characterization of MΦNPs

The hydrodynamic size and zeta potential were measured with dynamic light scattering (ZEN 3600 Zetasizer, Malvern). Transmission electron spectroscopy (FEI 200 kV Sphera) was used for visualizing the morphology of the nanoparticles stained with uranyl acetate (0.2 wt %). MΦNPs were also observed under a fluorescence microscope (EVOS FL) to identify cell membrane and the PLGA cores.

Synthesis of the algae-MΦNP-robot

Green algae were washed five times using ultrapure water with centrifugation at 500*g* for 3 min. The algae were adjusted to 1×10^7/ml. Then, 1 ml of algae was added to 4 μl of 10 mM DBCO-PEG_4-NHS ester (Click Chemistry Tools) and vortex-incubated at RT (22°C) and 700 rpm for 1 hour. Simultaneously, 1 ml of MΦNPs (1 mg/ml) in water was added to 4 μl of 10 mM azido-PEG_4-NHS ester (Click Chemistry Tools), and the sample was incubated at RT (22°C) for 1 hour. After the incubation, DBCO-labeled algae and azido-labeled MΦNPs were washed again in ultrapure water. The washings were performed by centrifugation at 500*g* for 2 min for green algae and at 16,100*g* for 3 min for MΦNPs. This washing step was repeated five times for each sample to ensure thorough removal of excess reagents. The conjugation was carried out by mixing DBCO-labeled green algae with azido-labeled MΦNPs for 1 hour at RT (22°C). After conjugation, the resulting product was washed three times with ultrapure water using centrifugation at 500*g* for 2 min. Last, the MΦNP-conjugated green algae (algae-MΦNP-robot) were kept in ultrapure water for further characterization. After incubation with 0.5 M acetic acid, the deflagellated green algae were used following a similar procedure for MΦNP conjugation (static algae-MΦNPs).

Characterization of the algae-MΦNP-robot

To obtain SEM images of algae-MΦNP-robots, the samples were fixed by adding 5% glutaraldehyde (Sigma-Aldrich) with a 1:1 volume ratio and transferring to 4°C overnight. Then, the samples were washed three times with ultrapure water using centrifugation at 100*g* for 2 min and dried overnight. After being sputtered with palladium, algae-MΦNP-robots were characterized through SEM with an acceleration voltage of 3 kV (Zeiss Sigma 500 SEM instrument). Static algae-MΦNPs and bare algae were prepared and analyzed through the same method. Furthermore, for fluorescence-based characterization, fluorescence microscopy (EVOS FL) was conducted to examine the autofluorescence of green algae under the Cy5 channel, DiO-loaded PLGA cores under the green fluorescent protein (GFP) channel, and DiI-labeled J774A.1 membranes under the red fluorescent protein (RFP) channel, respectively.

Motion analysis

For the motility characterization of green algae before and after conjugation with MΦNPs, the bare algae and algae-MΦNP-robots were suspended in TAP culture medium, followed by measurement of the motion speed and motile ratio at RT (22°C) and BT (37°C). Then, algae-MΦNP-robots were transferred to ACF (pH ~7.8) (Biochemazone, BZ177) to study the motion behaviors (motion speed and motile ratio) at 0, 0.25, 0.5, 1, 4, and 12 hours at both RT (22°C) and BT (37°C). Furthermore, to observe the influence of cytokines on the motility of algae-MΦNP-robots, they were washed into ACF containing specific cytokines: TNF-α (1 ng/ml; BioLegend), IL-6 (10 ng/ml; BioLegend), IL-1β (10 ng/ml; BioLegend), and IFN-γ (3.5 ng/ml; BioLegend). The motion speed and motile ratio were collected at 0, 1, 2, 4, 8, and 12 hours at BT (37°C). The motion behaviors of the algae-MΦNP-robot before and after release from the capsule were analyzed in ACF at BT (37°C). All motion videos were

taken by the Nikon Eclipse Ti-S/L100 inverted optical microscope with a digital camera (Hamamatsu, C11440) under ×10 objective lens (Nikon). The motion speed of unmodified or modified green algae at different conditions was determined by a NIS-Elements tracking module.

Algae viability examination

The viability of both unmodified and modified green algae was evaluated using a staining method with 5 μM SYTOX GFP (Thermo Fisher Scientific) (*46*). Specifically, the green algae, before and after conjugation with MΦNPs, were transferred to TAP culture medium and incubated at both RT (22°C) and BT (37°C). The samples were then mixed with SYTOX GFP, a fluorescent dye used to stain dead cells. For the viability evaluation of algae-MΦNP-robots in the presence of proinflammatory cytokine–containing ACF, the samples were collected and washed in ultrapure water using centrifugation at 500*g* for 3 min at 0, 1, 2, 4, 8, and 12 hours, followed by incubation with SYTOX GFP. To assess the viability of algae-MΦNP-robots from the stomach capsule or small intestine capsule, the green algae were first released from the respective capsules, collected from the stomach or small intestine into ACF, and then washed in ultrapure water using centrifugation at 500*g* for 3 min. Subsequently, the samples were incubated with SYTOX GFP. The viability of all green algae samples was calculated by counting the ratio of live and dead algae on an Invitrogen EVOS FL fluorescence microscope under the function of SYTOX GFP.

Characterization of proinflammatory cytokine receptors

For the MΦ membrane vesicle group, free-MΦNP group, algae-MΦNP-robot group, static algae-MΦNP group, and algae-MΦNP-robot released in ACF group, the samples were first quantified for MΦ membrane protein content (1 mg/ml) with a BCA assay (Life Technologies). For the bare algae group and algae-MΦNP-robot released in SGF groups, the samples were quantified to have the same concentration of green algae as the algae-MΦNP-robot group. All groups were followed by mixing with lithium dodecyl sulfate sample loading buffer (Invitrogen) to prepare the samples for electrophoresis. The prepared samples were loaded onto Bolt 4 to 12% bis-tris 12-well minigels (Invitrogen) in Mops running buffer (Invitrogen) for electrophoresis. To visualize the specific markers, Western blot assays were performed. The proteins involved in minigels were transferred to 0.45-μm nitrocellulose membranes (Pierce) with the use of Bolt transfer buffer (Novex) at 30 V for 60 min. The membranes were blocked using 3% bovine serum albumin (Sigma-Aldrich) in 1× PBS (Corning) and 0.05% Tween 20 (National Scientific). Anti-mouse primary antibodies, including TNF-R1 (Santa Cruz Biotechnology, H-5), IL-6Rα (Santa Cruz Biotechnology, D-8), IL-1Rl (Santa Cruz Biotechnology, H-8), and IFN-γRα (Santa Cruz Biotechnology, GIR-94), were used to probe signals on the membrane. The secondary staining was processed with corresponding horseradish peroxidase–conjugated immunoglobulin G antibodies (BioLegend). Chemiluminescence images were lastly developed with the Chemidoc MP Imaging System (Bio-Rad) to visualize and analyze the results of the Western blot assays.

In vitro proinflammatory cytokine neutralization

To study the dosage-dependent proinflammatory cytokine neutralization, 100 μl of algae-MΦNP-robots with different green algae concentrations, 0.125×10^7/ml (loading MΦNPs, 18.75 μg/ml), 0.25×10^7/ml (loading MΦNPs, 37.5 μg/ml), 0.5×10^7/ml (loading MΦNPs, 75 μg/ml), 1×10^7/ml (loading MΦNPs, 150 μg/ml), 2×10^7/ml (loading MΦNPs, 300 μg/ml), 4×10^7/ml (loading MΦNPs, 600 μg/ml), and 8×10^7/ml (loading MΦNPs, 1200 μg/ml), were mixed with TNF-α (0.5 ng/ml), IL-6 (2 ng/ml), IL-1β (2 ng/ml), and IFN-γ (1 ng/ml), respectively, in ultrapure water containing 10% FBS and then incubated at BT (37°C) for 2 hours. Then, we tested the neutralization ability of all groups in the mixture solution [containing TNF-α (0.5 ng/ml), IL-6 (2 ng/ml), IL-1β (2 ng/ml), and IFN-γ (1 ng/ml)] by following the same procedures. To further study the time-dependent proinflammatory cytokine neutralization ability with a higher concentration of proinflammatory cytokines, 100 μl of 4×10^7/ml (loading MΦNPs, 600 μg/ml) algae-MΦNP-robots was mixed with TNF-α (1 ng/ml), IL-6 (10 ng/ml), IL-1β (10 ng/ml), and IFN-γ (3.5 ng/ml) in ultrapure water containing 10% FBS and then incubated at BT (37°C) for 0, 1, 2, 4, 8, 12, and 24 hours, respectively. The free-MΦNP group, static algae-MΦNP group, and bare algae group were incubated with relevant dosage amounts and the same procedures. After the incubation, the remaining proinflammatory cytokines were collected from the supernatant by centrifuging at 16,100*g* for 10 min and then quantified with the enzyme-linked immunosorbent assay (ELISA) kit (BioLegend). All groups were performed with $n = 3$.

Preparation and characterization of the algae-MΦNP-robot capsule

The capsules were purchased from Torpac (mouse-specific size M gel). To load green algae samples into the capsule, hydrophobic coating was performed on the inner side of the capsule body and cap. This hydrophobic coating was achieved by preparing 4% (w/w) OTMS (Tokyo Chemical Industry) solutions in pure ethanol, filling the capsule cap or body with ~3 μl of the OTMS solutions using a primed syringe pump, and then incubating the capsules in an oven at 120°C for 1 hour to evaporate the solvent and form the hydrophobic layer. To ensure stability, this coating process was repeated 10 times. After the algae-MΦNP-robot encapsulation, the capsule body was gently filled with 2 μl of 1×10^9/ml (loading MΦNPs: 15 mg/ml) of the samples in ultrapure water with the primed syringe pump and covered with the capsule cap. To protect the green algae capsule from the harsh stomach environment, the Eudragit S-100 (Evonik Industries) enteric polymer was coated onto the outside layer of the capsule. Specifically, the enteric coating originates were prepared by mixing 1 g of S-100 powder into 10 ml of pure ethanol and stirring with 700 rpm at RT (22°C) overnight. Then, the green algae capsules were coated with the enteric protection layers through a dip-coating method and solvent evaporation at RT (22°C) for 25 min. The process was repeated five times to achieve the required protection function. The static algae-MΦNP capsules were prepared by following the same procedures. To simulate the capsule function in vivo, the green algae capsules were immersed into SGF (pH 1.5; RICCA Chemical) or ACF (pH 7.8; Biochemazone, BZ177) with 700 rpm of stirring at BT (37°C). The release profiles of the algae from the capsules were quantified by a Tecan Infinite M200 plate reader. The ex vivo release studies of algae capsules collected from the mouse stomach or small intestine were performed in ACF under the same conditions.

Animal care

The mice used in this study were housed in an animal facility at the University of California San Diego (UCSD) that complied with

federal, state, local, and National Institutes of Health (NIH) guidelines. Six-week-old male C57BL/6 mice were ordered from the Jackson Laboratory and maintained with standard housing specifications, including 12-hour light and 12-hour dark cycles, appropriate temperature, and suitable humidity. All animal experiments were conducted in accordance with the guidelines set, including pain reduction and humane euthanasia procedures by the NIH. In addition, these experiments were approved by the Institutional Animal Care and Use Committee of UCSD.

Pharmacokinetics and biodistribution analysis

Algae-MΦNP-robots (DiR-loaded in MΦNPs) were encapsulated, with each capsule containing 2×10^6 green algae robots (loading MΦNPs, 300 μg). These capsules were orally administered to 7-week-old male C57BL/6 mice with a capsule dosing syringe (Braintree Scientific). To evaluate the capsule protective function during passage through the stomach, mice were euthanized at 30 min or 2 hours after oral gavage, and their entire GI system was collected. Ex vivo GI fluorescence images were obtained by the Xenogen IVIS 200 system to quantify capsule integrity. The intact capsules were separated from the stomach or small intestine, respectively, to evaluate the motility and viability of loaded green algae in vitro. For biodistribution and retention studies, the mice were euthanized at 5, 7, 9, and 12 hours after administration, and the entire GI tract was collected, rinsed three times with 1× PBS, and subjected to ex vivo GI fluorescence imaging. Quantitative analysis was performed on the collected GI tracts using a Tecan Infinite M200 plate reader (Tecan; ex/em = 748/780 nm). A control group with static algae-MΦNP capsule was included in the study, and all groups had a sample size of $n = 3$ for statistical validity.

DSS-induced colitis in mice

Six-week-old male C57BL/6 mice were divided into groups of six mice per cage and acclimatized for 1 week before starting the in vivo experiments. For the prophylactic efficacy study, treatment started on day 0 and lasted for 10 days together with the DSS administration to induce the IBD condition. This experiment was mainly to explore whether algae-MΦNP-robot treatment could prevent the animals from forming DSS-induced IBD. Specifically, mice were administered 3% DSS (36 to 50 kDa; MP Biomedicals) supplemented in drinking water for 6 days, followed by normal water for 4 days. Throughout the 10-day treatment, mice in different groups were orally administered daily PBS (100 μl), an algae-MΦNP-robot capsule (2×10^6 green algae robots with 300 μg of MΦNPs per capsule), a static algae-MΦNP capsule (2×10^6 static green algae with 300 μg of MΦNPs per capsule), or algae-MΦNP-robots without capsule (denoted as "algae-MΦNP-robot"; 2×10^6 green algae robots with 300 μg of MΦNPs per 100 μl). In parallel, healthy mice treated with PBS served as the baseline control. The administration was performed using a capsule dosing syringe at a dosage of one capsule per day for 10 days. For the delayed treatment efficacy study, mice were first administered 3% DSS supplemented in their drinking water for 6 days and then replaced with regular drinking water for the remaining 4 days. Starting from day 5, mice were orally administered daily with various treatment groups as previously mentioned until day 9. The rationale for this experiment was mainly to explore whether algae-MΦNP-robot treatment could mitigate and recover the symptoms of IBD that had already developed.

Disease severity analysis

Throughout all the studies, daily changes in body weights of the mice were recorded during the experimental period. In addition, fecal samples were collected at predetermined time points to determine the DAI, which was based on the following characteristics: stool consistency (scored from 0 to 4), rectal bleeding (scored from 0 to 4), and weight loss (scored from 0 to 4) (*47*). At the study end points, the mice were euthanized. The entire colon was extracted, and its length was recorded. From the distal section of the colon, three pieces of colonic tissue (each measuring 0.5 cm in length, with a sample size of $n = 6$) were excised for histological analysis, immunofluorescence staining, and mRNA quantification, respectively. The remaining colonic tissue was weighed and homogenized in 0.5 ml of 1× PBS for the quantification of proinflammatory cytokine concentration. The homogenized samples were then centrifuged at 16,100*g* for 10 min at 4°C, and the concentration of TNF-α, IL-6, IL-1β, and IFN-γ in the supernatant was quantified using an ELISA kit (BioLegend).

Histological analysis of mouse colonic tissues

The collected colon samples ($n = 6$) proceeded to H&E staining and TUNEL staining at UCSD Histology Core. The histological samples were then assessed and scored on the basis of the presence and severity of various characteristics, including evaluation of neutrophilic and mononuclear infiltrates (scored from 0 to 3), epithelial architecture damage (scored from 0 to 3), muscle thickening (scoring from 0 to 3), goblet cell depletion (scoring from 0 to 1), and crypt abscess (scoring from 0 to 1) (*48*). The individual scores for each characteristic were summed, resulting in a colonic histological damage score ranging from 0 to 11 for each sample.

In vivo immunofluorescence imaging

For immunofluorescence imaging of ZO-1 and occludin tight junction proteins on mouse colonic tissues, 0.5-cm colonic tissues were fixed in Tissue-Tek O.C.T. compound (Sakura Finetek) and frozen-sectioned at −80°C. Before immunofluorescence staining, the colonic tissue samples were permeabilized with 0.25% Trition X-100 and blocked with PBS containing 2% bovine serum albumin for 1 hour. After blocking, the samples were then stained with mouse anti–ZO-1 antibodies (5 μg/ml) conjugated with Alexa Fluor 488 (Thermo Fisher Scientific) and mouse anti-occluding antibodies (1 μg/ml) conjugated with Alexa Fluor 594 (Thermo Fisher Scientific) overnight at 4°C. For nucleus staining, the samples were stained with Hoechst 33342 (1 μg/ml; Thermo Fisher Scientific) for 15 min at RT (22°C). Last, the immunofluorescence signals were observed using a confocal microscope (Leica SP8).

Quantitative reverse transcription polymerase chain reaction

After the acquisition of mouse colonic tissues, RNA was extracted using the Direct-zol RNA Miniprep kit (Zymo Research) on the basis of the manufacturer's protocol. The reverse transcription of the extracted RNA was performed using the ProtoScript First Strand cDNA Synthesis kit (New England Biolabs). After reverse transcription, quantitative reverse transcription polymerase chain reaction (qRT-PCR) was conducted using LUNA Universal qPCR Master Mix (New England Biolabs) with thermal cycling conditions of 95°C for 1 min, 40 cycles of 95°C for 15 s, and 60°C for 45 s. β-Actin was used as the reference gene. The primers used for

amplifications included the following: ZO-1, CTTCTCTTGCTG-GCCCTAAAC (forward) and TGGCTTCACTTGAGGTTTCTG (reverse); occludin, CACACTTGCTTGGGACAGAG (forward) and TAGCCATAGC-CTCCATAGCC (reverse); and β-actin, AAGTGTGACGTTGACATCCG (forward) and GATCCACATCT-GCTGGAAGG (reverse). All sequences refer to 5′ to 3′.

In vivo safety studies

For in vivo biosafety studies, 6-week-old male C57BL/6 mice were divided into groups of three mice per cage and acclimatized for 1 week before the in vivo experiments. From days 0 to 9, mice in different groups received daily oral administration of either 1× PBS (100 μl) or algae-MΦNP-robot capsules (2×10^6 green algae robots per capsule) using a capsule dosing syringe at a dosage of one capsule per day. The changes in body weights of all mice were recorded on a daily basis throughout the study. At the end of the study (day 10), the mice were euthanized for sample collection. For blood chemistry analysis and blood cell counts, each mouse's whole blood was collected in potassium-EDTA collection tubes (Sarstedt). This procedure was performed by the UCSD Animal Care Program Diagnostic Services Laboratory. For the histological analysis, the collected colon samples were carefully sectioned and stained with H&E using equipment from Leica Biosystems. After staining, the samples were imaged using a Nanozoomer 2.0-HT slide scanning system from Hamamatsu. The remaining colonic tissue was weighed and homogenized in 0.5 ml of 1× PBS for the quantification of proinflammatory cytokine concentration. The homogenized samples were then centrifuged at 16,100*g* for 10 min at 4°C, and the concentration of TNF-α, IL-6, IL-1β, and IFN-γ in the supernatant was quantified using an ELISA kit (BioLegend).

Statistical analysis

The experiments conducted were all performed repeatedly and independently to acquire the data shown in the figures, which are reported as error bars, representing ±SD relative to the mean. To assess the statistical significance between two groups, a two-tailed Student's *t* test was used, and for multiple comparisons, a one-way analysis of variance (ANOVA) with Dunnett's test was performed. Statistical significance is denoted as $*P < 0.05$, $**P < 0.01$, $***P < 0.001$, and $****P < 0.0001$. To minimize any potential bias that might occur during the study, no data were excluded, samples were allocated randomly to different experimental groups, organisms were cultured under the same environmental conditions and randomly allocated to each group, and investigators were not blinded during data collection and analysis throughout the experiments.

Supplementary Materials

This PDF file includes:
Figs. S1 to S26

Other Supplementary Material for this manuscript includes the following:
Movies S1 to S4

REFERENCES AND NOTES

1. S. Citi, Intestinal barriers protect against disease. *Science* **359**, 1097–1098 (2018).
2. J. R. Turner, Intestinal mucosal barrier function in health and disease. *Nat. Rev. Immunol.* **9**, 799–809 (2009).
3. E. V. Loftus Jr., Clinical epidemiology of inflammatory bowel disease: Incidence, prevalence, and environmental influences. *Gastroenterol* **126**, 1504–1517 (2004).
4. C. A. Dinarello, Proinflammatory cytokines. *Chest* **118**, 503–508 (2000).
5. J. J. O'Shea, A. Ma, P. Lipsky, Cytokines and autoimmunity. *Nat. Rev. Immunol.* **2**, 37–45 (2002).
6. M. Friedrich, M. Pohin, F. Powrie, Cytokine networks in the pathophysiology of inflammatory bowel disease. *Immunity* **50**, 992–1006 (2019).
7. M. F. Neurath, Cytokines in inflammatory bowel disease. *Nat. Rev. Immunol.* **14**, 329–342 (2014).
8. Y. R. Na, M. Stakenborg, S. H. Seok, G. Matteoli, Macrophages in intestinal inflammation and resolution: A potential therapeutic target in IBD. *Nat. Rev. Gastroenterol. Hepatol.* **16**, 531–543 (2019).
9. A. B. Pithadia, S. Jain, Treatment of inflammatory bowel disease (IBD). *Pharmacol. Rep.* **63**, 629–642 (2011).
10. C. N. Bernstein, Treatment of IBD: Where we are and where we are going. *Am. J. Gastroenterol.* **110**, 114–126 (2015).
11. D. S. Wilson, G. Dalmasso, L. Wang, S. V. Sitaraman, D. Merlin, N. Murthy, Orally delivered thioketal nanoparticles loaded with TNF-α–siRNA target inflammation and inhibit gene expression in the intestines. *Nat. Mater.* **9**, 923–928 (2010).
12. A. Stallmach, S. Hagel, T. Bruns, Adverse effects of biologics used for treating IBD. *Best Pract. Res. Clin. Gastroenterol.* **24**, 167–182 (2010).
13. F. Mehta, Report: Economic implications of inflammatory bowel disease and its management. *Am. J. Manag. Care* **22**, 51–60 (2016).
14. J. Wang, *Nanomachines: Fundamentals and Applications* (John Wiley & Sons, 2013).
15. A. C. Hortelao, C. Simó, M. Guix, S. Guallar-Garrido, E. Julián, D. Vilela, L. Rejc, P. Ramos-Cabrer, U. Cossío, V. Gómez-Vallejo, T. Patiño, J. Llop, S. Sánchez, Swarming behavior and in vivo monitoring of enzymatic nanomotors within the bladder. *Sci. Robot.* **6**, eabd2823 (2021).
16. Y. Dong, L. Wang, V. Iacovacci, X. Wang, L. Zhang, B. J. Nelson, Magnetic helical micro-/nanomachines: Recent progress and perspective. *Matter* **5**, 77–109 (2022).
17. C. K. Schmidt, M. Medina-Sánchez, R. J. Edmondson, O. G. Schmidt, Engineering microrobots for targeted cancer therapies from a medical perspective. *Nat. Commun.* **11**, 5618 (2020).
18. Z. Wu, L. Li, Y. Yang, P. Hu, Y. Li, S. Y. Yang, L. V. Wang, W. Gao, A microrobotic system guided by photoacoustic computed tomography for targeted navigation in intestines in vivo. *Sci. Robot.* **4**, eaax0613 (2019).
19. J. Li, B. Esteban-Fernández de Ávila, W. Gao, L. Zhang, J. Wang, Micro/nanorobots for biomedicine: Delivery, surgery, sensing, and detoxification. *Sci. Robot.* **2**, eaam6431 (2017).
20. H. Wang, M. Pumera, Fabrication of micro/nanoscale motors. *Chem. Rev.* **115**, 8704–8735 (2015).
21. E. Kim, S. Jeon, H. K. An, M. Kianpour, S. W. Yu, J. Y. Kim, J. C. Rah, H. Choi, A magnetically actuated microrobot for targeted neural cell delivery and selective connection of neural networks. *Sci. Adv.* **6**, eabb5696 (2020).
22. F. Zhang, Z. Li, C. Chen, H. Luan, R. H. Fang, L. Zhang, J. Wang, Biohybrid microalgae robots: Design, fabrication, materials and applications. *Adv. Mater.* **36**, 2303714 (2023).
23. X. Yan, Q. Zhou, M. Vincent, Y. Deng, J. Yu, J. Xu, T. Xu, T. Tang, L. Bian, Y. J. Wang, K. Kostarelos, L. Zhang, Multifunctional biohybrid magnetite microrobots for imaging-guided therapy. *Sci. Robot.* **2**, eaaq1155 (2017).
24. V. M. Kadiri, C. Bussi, A. W. Holle, K. Son, H. Kwon, G. Schütz, M. G. Gutierrez, P. Fischer, Biocompatible magnetic micro- and nanodevices: Fabrication of FePt nanopropellers and cell transfection. *Adv. Mater.* **32**, e2001114 (2020).
25. B. Dai, J. Wang, Z. Xiong, X. Zhan, W. Dai, C. C. Li, S. P. Feng, J. Tang, Programmable artificial phototactic microswimmer. *Nat. Nanotechnol.* **11**, 1087–1092 (2016).
26. L. Ren, W. Wang, T. E. Mallouk, Two forces are better than one: Combining chemical and acoustic propulsion for enhanced micromotor functionality. *Acc. Chem. Res.* **51**, 1948–1956 (2018).
27. J. Liang, K. Liang, Biocatalytic metal–organic frameworks: Prospects beyond bioprotective porous matrices. *Adv. Funct. Mater.* **30**, 2001648 (2020).
28. Z. Lin, C. Gao, D. Wang, Q. He, Bubble-propelled Janus gallium/zinc micromotors for the active treatment of bacterial infections. *Angew. Chem. Int. Ed. Engl.* **60**, 8750–8754 (2021).
29. R. Mundaca-Uribe, E. Karshalev, B. Esteban-Fernández de Ávila, X. Wei, B. Nguyen, I. Litvan, R. H. Fang, L. Zhang, J. Wang, A microstirring pill enhances bioavailability of orally administered drugs. *Adv. Sci.* **8**, 2100389 (2021).
30. O. Felfoul, M. Mohammadi, S. Taherkhani, D. De Lanauze, Y. Z. Xu, D. Loghin, S. Essa, S. Jancik, D. Houle, M. Lafleur, L. Gaboury, M. Tabrizian, N. Kaou, M. Atkin, T. Vuong, G. Batist, N. Beauchemin, D. Radzioch, S. Martel, Magneto-aerotactic bacteria deliver drug-containing nanoliposomes to tumour hypoxic regions. *Nat. Nanotechnol.* **11**, 941–947 (2016).
31. Y. Alapan, O. Yasa, O. Schauer, J. Giltinan, A. F. Tabak, V. Sourjik, M. Sitti, Soft erythrocyte-based bacterial microswimmers for cargo delivery. *Sci. Robot.* **3**, eaar4423 (2018).
32. L. Sun, Y. Yu, Z. Chen, F. Bian, F. Ye, L. Sun, Y. Zhao, Biohybrid robotics with living cell actuation. *Chem. Soc. Rev.* **49**, 4043–4069 (2020).

33. F. Zhang, J. Zhuang, Z. Li, H. Gong, B. Esteban-Fernández de Ávila, Y. Duan, Q. Zhang, J. Zhou, L. Yin, E. Karshalev, W. Gao, V. Nizet, R. H. Fang, L. Zhang, J. Wang, Nanoparticle-modified microrobots for in vivo antibiotic delivery to treat acute bacterial pneumonia. *Nat. Mater.* **21**, 1324–1332 (2022).
34. O. Yasa, P. Erkoc, Y. Alapan, M. Sitti, Microalga-powered microswimmers toward active cargo delivery. *Adv. Mater.* **30**, e1804130 (2018).
35. H. Kurtuldu, J. S. Guasto, K. A. Johnson, J. P. Gollub, Enhancement of biomixing by swimming algal cells in two-dimensional films. *Proc. Natl. Acad. Sci. U.S.A.* **108**, 10391–10395 (2011).
36. F. Zhang, Z. Li, Y. Duan, H. Luan, L. Yin, Z. Guo, C. Chen, M. Xu, W. Gao, R. H. Fang, L. Zhang, J. Wang, Extremophile-based biohybrid micromotors for biomedical operations in harsh acidic environments. *Sci. Adv.* **8**, eade6455 (2022).
37. J. Shao, M. Abdelghani, G. Shen, S. Cao, D. S. Williams, J. C. van Hest, Erythrocyte membrane modified janus polymeric motors for thrombus therapy. *ACS Nano* **12**, 4877–4885 (2018).
38. F. Zhang, R. Mundaca-Uribe, N. Askarinam, Z. Li, W. Gao, L. Zhang, J. Wang, Biomembrane-functionalized micromotors: Biocompatible active devices for diverse biomedical applications. *Adv. Mater.* **34**, e2107177 (2022).
39. C. M. J. Hu, R. H. Fang, K. C. Wang, B. T. Luk, S. Thamphiwatana, D. Dehaini, P. Nguyen, P. Angsantikul, C. H. Wen, A. V. Kroll, C. Carpenter, M. Ramesh, V. Qu, S. H. Patel, J. Zhu, W. Shi, F. M. Hofman, T. C. Chen, W. Gao, K. Zhang, S. Chien, L. Zhang, Nanoparticle biointerfacing by platelet membrane cloaking. *Nature* **526**, 118–121 (2015).
40. A. Parodi, N. Quattrocchi, A. L. van de Ven, C. Chiappini, M. Evangelopoulos, J. O. Martinez, B. S. Brown, S. Z. Khaled, I. K. Yazdi, M. V. Enzo, L. Isenhart, M. Ferrari, E., Synthetic nanoparticles functionalized with biomimetic leukocyte membranes possess cell-like functions. *Nat. Nanotechnol.* **8**, 61–68 (2013).
41. Q. Zhang, D. Dehaini, Y. Zhang, J. Zhou, X. Chen, L. Zhang, R. H. Fang, W. Gao, L., Neutrophil membrane-coated nanoparticles inhibit synovial inflammation and alleviate joint damage in inflammatory arthritis. *Nat. Nanotechnol.* **13**, 1182–1190 (2018).
42. S. Thamphiwatana, P. Angsantikul, T. Escajadillo, Q. Zhang, J. Olson, B. T. Luk, S. Zhang, R. H. Fang, W. Gao, V. Nizet, L. Zhang, Macrophage-like nanoparticles concurrently absorbing endotoxins and proinflammatory cytokines for sepsis management. *Proc. Natl. Acad. Sci. U.S.A.* **114**, 11488–11493 (2017).
43. J. D. Cox, M. S. Curry, S. K. Skirboll, P. L. Gourley, D. Y. Sasaki, Surface passivation of a microfluidic device to glial cell adhesion: A comparison of hydrophobic and hydrophilic SAM coatings. *Biomaterials* **23**, 929–935 (2002).
44. F. Zhang, Z. Li, Y. Duan, A. Abbas, R. Mundaca-Uribe, L. Yin, H. Luan, W. Gao, R. H. Fang, L. Zhang, J. Wang, Gastrointestinal tract drug delivery using algae motors embedded in a degradable capsule. *Sci. Robot.* **7**, eabo4160 (2022).
45. A. M. Dos Santos, S. G. Carvalho, A. B. Meneguin, R. M. Sábio, M. P. D. Gremião, M. Chorilli, Oral delivery of micro/nanoparticulate systems based on natural polysaccharides for intestinal diseases therapy: Challenges, advances and future perspectives. *J. Control. Release* **334**, 353–366 (2021).
46. M. Sato, Y. Murata, M. Mizusawa, H. Iwahashi, S. I. Oka, A simple and rapid dual fluorescence viability assay for microalgae. *Microbiol. Cult. Coll.* **20**, 53–59 (2004).
47. J. J. Kim, M. S. Shajib, M. M. Manocha, W. I. Khan, Investigating intestinal inflammation in DSS-induced model of IBD. *J. Vis. Exp.* **60**, 3678 (2012).
48. S. Das, A. Sarkar, S. S. Choudhury, K. A. Owen, V. Castillo, S. Fox, L. Eckmann, M. R. Elliott, J. E. Casanova, P. B. Ernst, Engulfment and cell motility protein 1 (ELMO1) has an essential role in the internalization of *Salmonella* Typhimurium into enteric macrophages that impact disease outcome. *Cell Mol. Gastroenter.* **1**, 311–324 (2015).

Acknowledgments

Funding: This work is supported by the Defense Threat Reduction Agency Joint Science and Technology Office for Chemical and Biological Defense under grant number HDTRA1-21-1-0010. **Author contributions:** Z.L., Y.D., F.Z., L.Z., and J.W. conceived the study and designed the experiments. Z.L., Y.D., and F.Z. performed and conducted the experiments. Z.L., Y.D., F.Z., H.L., W.-T.S., Y.Y., N.X., Z.G., E.Z., L.Y., R.H.F., W.G., L.Z., and J.W. discussed and analyzed the data. Z.L., Y.D., F.Z., H.L., W.G., L.Z., and J.W. wrote the manuscript. All the authors reviewed, edited, and approved the paper. **Competing interests:** The authors declare that they have no competing interests. **Data and materials availability:** All data needed to evaluate the conclusions in the paper are present in the paper or the Supplementary Materials. The original dataset was uploaded to the Dryad system with the following DOI: 10.5061/dryad.2rbnzs7x9.

Submitted 4 October 2023
Accepted 30 May 2024
Published 26 June 2024
10.1126/scirobotics.adl2007

Science Robotics

Biohybrid microrobots regulate colonic cytokines and the epithelium barrier in inflammatory bowel disease

Zhengxing Li, Yaou Duan, Fangyu Zhang, Hao Luan, Wei-Ting Shen, Yiyan Yu, Nianfei Xian, Zhongyuan Guo, Edward Zhang, Lu Yin, Ronnie H. Fang, Weiwei Gao, Liangfang Zhang, and Joseph Wang

Sci. Robot. **9** (91), eadl2007. DOI: 10.1126/scirobotics.adl2007

Editor's summary

Regulating cytokine activity can effectively manage inflammatory bowel disease, but traditional treatments are immunosuppressant or only target specific cytokines. By combining the robust motion of green algae with the binding abilities of macrophage membrane–coated nanoparticles, Li *et al.* developed a biohybrid microrobot that captured and removed a range of proinflammatory cytokines in vitro. The algae-based robots were encapsulated for protective passage through the stomach and administered to mice. In vivo studies confirmed biosafety and successful prevention and treatment of inflammatory bowel disease in a mouse model. The algae-based robots also hold potential for treatment of other cytokine-related disorders. —Melisa Yashinski